22nd International Conference on Renewable Energies and Power Quality (ICREPQ'24)
Bilbao (Spain), 26th to 28th June 2024
Renewable Energy and Power Quality Journal (RE&PQJ)
ISSN 2172-038 X, Volume No.22, September 2024

Subsea DC power cable modelling and computational validation

Frederico Oliveira Passos[1], José Maria de Carvalho Filho[1], José Carlos de Oliveira[2], Christel Enock Ghislain Ogoulola[1], Alex Reis[3], José Mauro Teixeira Marinho[4]

[1] Federal University of Itajubá
37500903 – Itajubá, MG – Brazil – P.O. Box: 50
Phone number: +55 (35) 3629-1788

[2] University of Uberlândia
38408100 – Uberlândia, MG – Brazil – P.O. Box: 593 Phone number: +55 (34) 32394707

[3] University of Brasília
72444240 – Brasília, DF - Brazil - P.O. Box: 593
Phone number: +55 (61) 31078901

[4] Petrobras S.A. Company
219419115 – Rio de Janeiro, RJ – Brazil, 950
Phone number: +55 (21) 3224-4477

Abstract. The growing number of applications involving the transmission of electrical energy from AC sources for the purpose of interconnecting onshore/offshore AC networks has motivated several investigations to define the most appropriate topological and parametric structures for the purposes in question. In this scenario, the issue of electrical supplies for platforms for oil extraction arises to reduce greenhouse gases produced by local generation units. The strategies used may consist of AC or DC transmission systems, being the latter and attractive from the point of view of technical and operational feasibility. A DC interconnection complex comprises several units, among which the submarine cables stand out. For carrying out performance studies of the system as a whole, the performance assessments require, in addition to the sending and receiving converter stations, DC interconnection cable reliable models. To this end, together with propositions of equivalent circuits and their representative parameters, this article carries out a comparative computational analysis of the calculated parameters with those commercially available.

Key words. HVDC transmission, subsea DC cables, oil and gas platforms, offshore renewable energy installations.

1. Introduction

In recent years, the global energy landscape has undergone a significant shift towards the use of renewable energy sources and the exploration of offshore resources. This shift has led to the need for advancements in power transmission technologies to efficiently transport energy from power stations to the main electrical grids. In this context, the HVDC transmission strategy has become an attractive solution for offshore [1], [2]. In fact, the interconnections of offshore wind farms, as well as the supply of offshore loads throughout HVDC arrangements has emerged as a possible solution for interconnections between electrical areas. In this context, the use of submarine cables is essential for the enterprise in enhancing the overall efficiency and reliability of the energy network.

Offshore renewable energy installations, such as wind farms, are now being located in areas with plentiful and consistent wind resources, often at a considerable distance from the shore. Considering the power levels to be transported and the distances involved, traditional HVAC transmission presents operational limitations and high losses. On the other hand, HVDC technology offers clear advantages, making it attractive for its purposes [3].

Once the strategy for energy transmission has been established, it is imperative that studies be carried out on the performance of the installation, both in terms of its steady state operating regime, as well the dynamic and electromagnetic operational conditions. To this end, the need for reliable models for the complex as a whole is recognized and, among the parts, the issue focused on in this article arises, that is, submarine cables [4]. Accurate calculation of their electrical parameters, based on both the cable's physical properties and material, is crucial to ensure the proper functionality of the overall system [5].

It is important to highlight that the determination of equivalent parameters representing cables is a topic of great relevance for electrical studies involving steady-state, transient, dynamic operating conditions, and fault conditions [6]. Although the article is focused on these issues, other operational situations imposed on the cable are also necessary, such as thermal aspects [7].

The strategy utilized in this article involves defining the geometric and physical characteristics of cables, focusing on the conductive area, insulation layers, dielectric properties, shielding, and grounding connections. These data are then implemented into the PSCAD and EMTP-RV software for analysis. PSCAD offers modelling tools using two analysis methods, while EMTP-RV uses the original formulation by Pollaczeck. These tools are valuable for determining the parameters of insulated cables, such as resistance, inductance, and capacitance, essential for studying energy transfer solutions. Additionally, a computational resource was developed using basic formulations by Pollaczeck, Wedepohl, Saad, Lima, and Bianchi to determine the equivalent parameters. By combining these approaches, the study aimed to establish and correlate the necessary quantities for the research presented in this article.

The results arising from this calculation strategy are then compared with information from manufacturers, thus enabling a process of validating the proposition for the models included in this work. To achieve these objectives, Section 2 provides the mathematical formulation for calculating the R, L, C parameters of unipolar (SC) cables in the frequency domain. In section 3, the results of the computer simulation for a 150 kV DC cable are presented, thus enabling a ready correlation with the data provided by manufacturers. Finally, Section 4 summarizes the results of the analyses carried out in this work.

2. Mathematical Formulation

A. *Single core cable internal impedance matrix*

To establish the electrical parameters, the equations governing the equivalent performance of a submarine power cable, with one single core, can be represented by loop equations, as represented in Figure 1. The so-called Loop 1 represents the physical arrangement of the conductor to the sheath, the Loop 2 corresponds to the one from the sheath to the armour, and Loop 3 denotes the loop from the armour to the sea. It is worth mentioning that the unipolar cable has three conductors (four when including seawater) and three insulating layers, which are not shown in Figure 1.

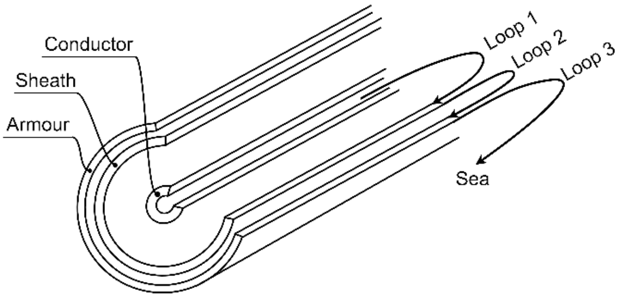

Fig.1. Single-core subsea cable cross sections.

The DC cable can be represented by an equivalent circuit, as shown in Figure 2. This representation takes into account the effects of three circulating currents: the one that flows through the central conductor and returns through the sheath, the second from the sheath and returns through the armature, and the third, of the sheath returning by sea. In the Figure, V_i and I_i with i ∈{1,2,3} are the voltages and currents per unit length for loops 1, 2 and 3, respectively.

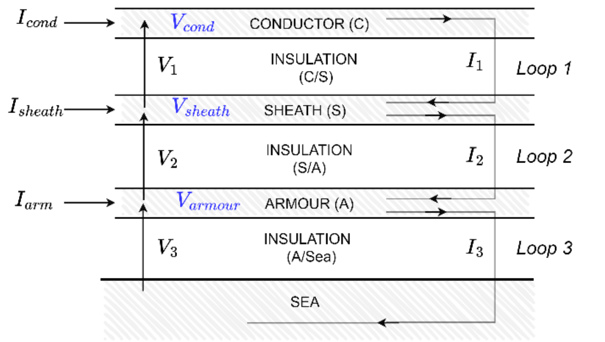

Fig.2. Impedance equivalent circuit.

Applying Kirchhoff's law, the mathematical relationships that govern the electrical quantities associated with the conductor's core, sheath, and armature are established through (1).

$$\begin{bmatrix} V_1 \\ V_2 \\ V_3 \end{bmatrix} = \underbrace{\begin{bmatrix} Z_{11} & Z_{12} & 0 \\ Z_{21} & Z_{22} & Z_{23} \\ 0 & Z_{32} & Z_{33} \end{bmatrix}}_{Z_L} \cdot \begin{bmatrix} I_1 \\ I_2 \\ I_3 \end{bmatrix} \tag{1}$$

The elements of the matrix are given by (2).

$$\begin{cases} Z_{11} = Z_{ext-C} + Z_{ins-C/S} + Z_{int-S} \\ Z_{22} = Z_{ext-S} + Z_{ins-S/A} + Z_{int-A} \\ Z_{33} = Z_{ext-A} + Z_{ins-A/sea} + Z_{self-sea} + Z_{mut-sea} \\ Z_{12} = Z_{21} = -Z_{mut-S} \\ Z_{23} = Z_{32} = -Z_{mut-A} \end{cases} \tag{2}$$

The external impedances, per-unit of length of the conductor, sheath, and armature layers, Z_{ext-C}, Z_{ext-S}, and Z_{ext-A}, can be described by the equation (3).

$$Z_{ext} = \frac{\rho\sigma}{2\pi r_{ext}} \cdot \frac{I_o(\sigma r_{ext})K_1(\sigma r_{int}) + K_0(\sigma r_{ext})I_1(\sigma r_{int})}{I_1(\sigma r_{ext})K_1(\sigma r_{int}) - I_1(\sigma r_{int})K_1(\sigma r_{ext})} \tag{3}$$

Where:

$I_o(x)$ and $I_1(x)$ are the first kind modified Bessel functions of order 0 and 1 respectively;

$K_o(x)$ and $K_1(x)$ are the second kind modified Bessel functions of order 0 and 1 respectively;

$\sigma = \sqrt{j\omega\,\mu/\rho}$ is the complex propagation constant in the conducting layers;

r_{ext} and r_{int} are the external and internal radius of the conducting layer;

μ is the is the permeability of the conducting layer.

ρ is the resistivity of the conducting layer;

ω is the system angular frequency.

Likewise, the internal impedances, per unit length of the conductor, sheath and armature layers, denoted by Z_(int-S) and Z_(int-A), are defined by equation (4).

$$Z_{int} = \frac{\rho\sigma}{2\pi r_{ext}} \cdot \frac{I_o(\sigma r_{int})K_1(\sigma r_{ext}) + K_0(\sigma r_{int})I_1(\sigma r_{ext})}{I_1(\sigma r_{ext})K_1(\sigma r_{int}) - I_1(\sigma r_{int})K_1(\sigma r_{ext})} \tag{4}$$

The mutual impedances per-unit length of sheath and armour, Z_{mut-S} and Z_{mut-A}, are given by (5), where $\zeta = r_{ext} \cdot r_{int}$

$$Z_{mut} = \frac{\rho}{2\pi\zeta} \cdot \frac{1}{I_1(\sigma r_{ext})K_1(\sigma r_{int}) - I_1(\sigma r_{int})K_1(\sigma r_{ext})} \tag{5}$$

The impedance of the insulation between two conducting layers, $Z_{ins-C/S}$, $Z_{ins-S/A}$ and $Z_{ins-A/sea}$, can be established in (6).

$$Z_{ins} = j\omega \frac{\mu_{ins}}{2\pi} \ln\left(\frac{r_{out}}{r_{in}}\right) \tag{6}$$

Where:
μ_{ins} is the permeability of the insulation;
r_{out} and r_{in} are the outside and inside radius of insulation layer, respectively.

Considering the equation (2), the self and mutual return impedances $Z_{self-sea}$ and $Z_{mut-sea}$ need to be determined in order to establish the total series impedance of the cable. It is worth mentioning that simulation programs such as PSCAD and EMTP-RV use numerical models to calculate proper and mutual impedances for underground cables. Given that the objective of the article is focused on the comparative analysis of different models, general mathematical expressions will be established for Z_self and Z_mut for underground and submarine cables, respectively of Z_(int-S) and Z_(int-A) defined by (4).

B. *Ground return impedances of cable*

The equations determining loopback impedance were first derived by Pollaczeck for underground cables. This strategy was based on the hypothesis that the cable was buried in a semi-infinite earth, and also that the permeability of the earth μ is equal to μo. Under this assumption and for two identical cables with the same depth in relation to the earth, Pollaczeck's formulation for calculating the return to earth and the mutual impedances is given by (7) and (8), respectively, [8].

$$Z_{self} = \frac{j\omega\mu_o}{2\pi}\left[K_o(\sigma_g R) - K_o(\sigma_g D) + 2 \cdot J_s\right] \tag{7}$$

$$Z_{mut} = \frac{j\omega\mu_o}{2\pi}\left[K_o(\sigma_g \delta) - K_o(\sigma_g D') + 2 \cdot J_m\right] \tag{8}$$

Where $D = \sqrt{R^2 + 4h^2}$, $D' = \sqrt{\delta^2 + 4h^2}$, being R the overall radius of cable, h the depth, δ the horizontal distance between cables, μ_o the permeability of free space, σ_g the complex propagation constant in the soil, and J_s and J_m given by (9) and (10), respectively.

$$J_s = \int_0^\infty \frac{e^{\left(-2h\cdot\sqrt{\lambda^2+\sigma_g^2}\right)}}{|\lambda| + \sqrt{\lambda^2 + \sigma_g^2}} \cdot \cos(\lambda \cdot R)d\lambda \tag{9}$$

$$J_m = \int_0^\infty \frac{e^{\left(-2h\cdot\sqrt{\lambda^2+\sigma_g^2}\right)}}{|\lambda| + \sqrt{\lambda^2 + \sigma_g^2}} \cdot \cos(\lambda \cdot \delta)d\lambda \tag{10}$$

In order to reduce the computational complexity caused by evaluating the infinite Pollaczeck's integral for high frequency ranges, Wedepohl and Wilcox [9] developed an analytic approximation using (11) and (12). Under such condition, the cable's self and mutual return impedance formulation specifically is valid for frequencies that meet $|\sigma_g R| < 0.25$ and $|\sigma_g \delta| < 0.25$, respectively. The main advantages of using these formulas are solution stability and speed [9] being γ is the Euler's constant.

.

$$Z_{self} = \frac{j\omega\mu_o}{2\pi}\left[-\ln\left(\frac{\gamma\sigma_g R}{2}\right) + \frac{1}{2} - \frac{4}{3}\sigma_g h\right] \tag{11}$$

$$Z_{mut} = \frac{j\omega\mu_o}{2\pi}\left[-\ln\left(\frac{\gamma\sigma_g \delta}{2}\right) + \frac{1}{2} - \frac{4}{3}\sigma_g h\right] \tag{12}$$

On the other hand, Omar Saad and Giroux highlighted the complex nature of the infinite integral and proposed a simplified closed-form approximation for the self and mutual impedances of underground cables using (12) and (13). This allows for direct and easy assessment [10].

$$Z_{self} = \frac{j\omega\mu_o}{2\pi}\left[K_o(\sigma_g R) + \frac{2}{4 + \sigma_g^2 R^2} \cdot \mathrm{e}^{(-2h\sigma_g)}\right] \tag{12}$$

$$Z_{mut} = \frac{j\omega\mu_o}{2\pi}\left[K_o(\sigma_g \delta) + \frac{2}{4 + \sigma_g^2 \delta^2} \cdot \mathrm{e}^{(-2h\sigma_g)}\right] \tag{13}$$

Lima and Portela also developed an analysis of closed expressions for ground return impedance of underground cables, based on Pollaczeck's formulation (14) and (15). They used an approximate expression derived from the asymptotic expansion. This approximation is valid for cases where h > 2R [11].

$$Z_{self} = \frac{j\omega\mu_o}{2\pi}\left[K_o(\sigma_g R) + \alpha_1 K_2(\sigma_g D) - \alpha_2 e^{-2h\sigma_g}\right] \tag{14}$$

$$Z_{mut} = \frac{j\omega\mu_o}{2\pi}\left[K_o(\sigma_g \delta) + \alpha_3 K_2(\sigma_g D') - \alpha_4 e^{-2h\sigma_g}\right] \tag{15}$$

Where D and D' are the same parameter given in (7) and (8), $K_2(x)$ is the second kind modified Bessel functions of order 2, and α_1, α_2, α_3 and α_4 are given by (16).

$$\begin{cases} \alpha_1 = \dfrac{4h^2 - R^2}{D'^2} \\ \alpha_2 = 2 \cdot \left(\dfrac{4h^2 - R^2}{\sigma_g^2 \cdot D'^4}\right) \\ \alpha_3 = \dfrac{4h^2 - \delta^2}{D^2} \\ \alpha_4 = 2 \cdot \left(\dfrac{4h^2 - \delta^2}{\sigma_g^2 \cdot D^4}\right) \end{cases} \tag{16}$$

C. *Sea return impedances of cable*

As a simplifying hypothesis adopted to calculate the sea return impedance, Bianchi and Luoni [12] assumed that the cable is surrounded by an undefined sea of infinite radius when compared to the transverse dimensions of the cable. Under this assumption, the self and mutual impedance expressions of the DC cable are given by (17) and (18) [12].

$$Z_{self-sea} = \frac{\rho_{sea}\sigma_{sea}}{2\pi R} \cdot \frac{K_o(\sigma_{sea}R)}{K_1(\sigma_{sea}R)} \tag{17}$$

$$Z_{mut-sea} = \frac{\rho_{sea}\sigma_{sea}}{2\pi R} \cdot \frac{K_o(\sigma_{sea}\delta)}{K_1(\sigma_{sea}R)} \tag{18}$$

Where ρ_{sea} is the sea resistivity and $\sigma_{sea} = \sqrt{j\omega\mu_o/\rho_{sea}}$.

Finally, by considering (1) and referring to Figure 2, the conductor, sheath, and armour voltages may be obtained throughout (19).

$$\begin{bmatrix} V_{cond} \\ V_{sheath} \\ V_{arm} \end{bmatrix} = \underbrace{\begin{bmatrix} 1 & -1 & 0 \\ 0 & 1 & -1 \\ 0 & 0 & 1 \end{bmatrix}^{-1} \cdot Z_L \cdot \begin{bmatrix} 1 & 0 & 0 \\ 1 & 1 & 0 \\ 1 & 1 & 1 \end{bmatrix}}_{\begin{bmatrix} Z_{cc} & Z_{cs} & Z_{ca} \\ Z_{sc} & Z_{ss} & Z_{sa} \\ Z_{ac} & Z_{as} & Z_{aa} \end{bmatrix}} \cdot \begin{bmatrix} I_{cond} \\ I_{sheath} \\ I_{arm} \end{bmatrix} \tag{19}$$

According to [13], the armour of a submarine cable is generally of thickness to avoid water infiltration, therefore the armour voltages can be considered with earth potential at all points along the length of the cable. Also, the sheath voltages along the cable are very small when compared to the conductor voltage values. Under these conditions, the sheath voltages are also at ground potential. Thus, adopting the boundary condition $V_{sheath} = V_{arm} = 0$, the impedance matrix in (19) can be rewritten via (20), where β_1 and β_2 parameters are given by (21) and (22).

$$Z_{cable} = Z_{cc} + \beta_1 \cdot Z_{cs} + \beta_2 \cdot Z_{ca} \tag{20}$$

$$\beta_1 = \frac{Z_{sa} \cdot Z_{ac} - Z_{sc} \cdot Z_{aa}}{Z_{ss} \cdot Z_{aa} - Z_{sa} \cdot Z_{as}} \tag{21}$$

$$\beta_2 = \frac{Z_{sc} \cdot Z_{as} - Z_{ss} \cdot Z_{ac}}{Z_{ss} \cdot Z_{aa} - Z_{sa} \cdot Z_{as}} \tag{22}$$

The DC cable admittance can be expressed through (23), which only takes into account the susceptance being ε_r the permittivity of the insulation.

.

$$Y_{cable} = j\omega \cdot \frac{2\pi\varepsilon_r}{\ln\left(\frac{r_{out}}{r_{in}}\right)} \tag{23}$$

3. Computational Results and Comparison to Manufacturer Data

Figure 3 shows the cross section of two identical DC submarine cables for single our a bipolar symmetric HVDC system configuration. For the purpose of analysing the different previously established models, a 150 kV DC submarine cable was considered [13].

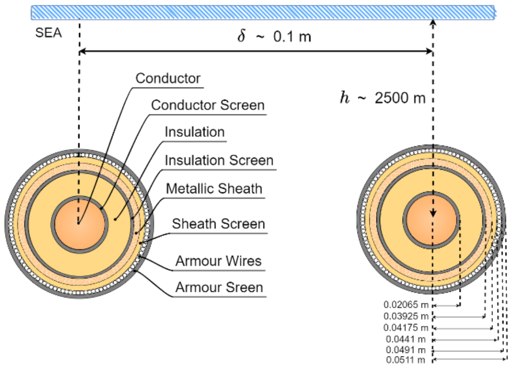

Fig.3. Physical structure of subsea DC cable.

The specific geometry and material properties data of the subsea DC cable in a moderate climate are provided in Table I [14].

Table I. – Subsea DC cable parameters [14].

Layer	Thickness [mm]	ρ [nΩm]	μ_r	ε_r
Conductor	18.96	17.2	1	-
Conductor Screen	1.7	-	1	2.3
Insulation (XLPE)	17	-	1	2.5
Insulation Screen	1.0	-	1	2.3
Metallic Sheath	2.5	220	1	-
Sheath Screen	2.5	-	1	2.3
Armour Wires	5	180	10	-
Armour Screen	2	-	1	-

Figure 4 illustrates the relationship between the cable's resistance and inductance at various frequencies for different return impedance models of a 150 kV subsea DC cable. The impedance calculations were carried out using the PTC MathCad© program. The DC cables are assumed to be buried on the seabed at a depth of 2500 m, with a horizontal distance of approximately 0.1 m between them. In Figure 4, only the low frequency part of the curves has been shown, as it is only at lower frequencies that the different formulations diverge.

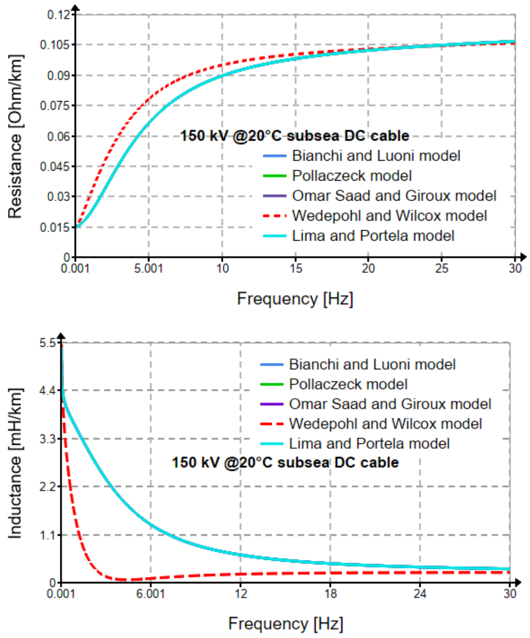

Fig.4. Resistance and inductance of DC cable (h = 2500 m).

The analysis revealed that the Wedepohl-Wilcox's approximation (see Section 2) is not suitable for calculating the submarine DC cables impedance at a depth of 2500 m, within the low frequency range. To this end the Wedepohl model has been compared to other DC cables models buried at depths of 300 m (see Figure 5) and 100 m (see Figure 6). Figure 6 shows that the results for DC power cables at a depth of 100 m are satisfactory. However, it is important to note that the Wedepohl-Wilcox model should not be used when considering the Bianchi and Luoni assumptions for sea return impedance calculations.

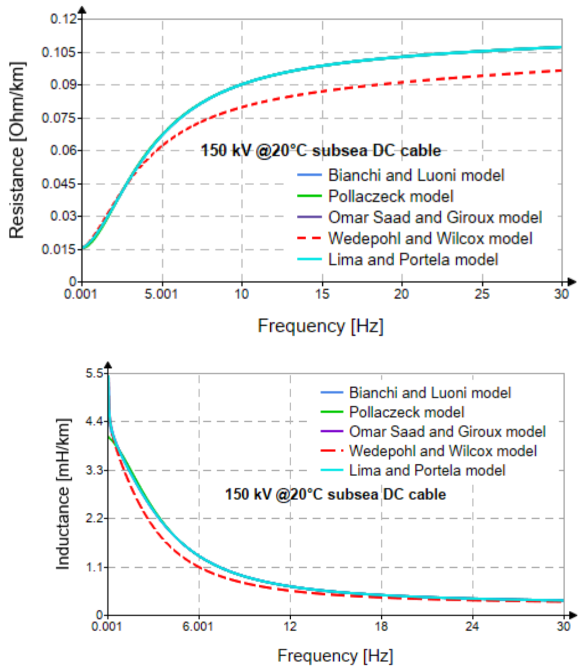

Fig.5. Resistance and inductance of DC cable (h = 300 m).

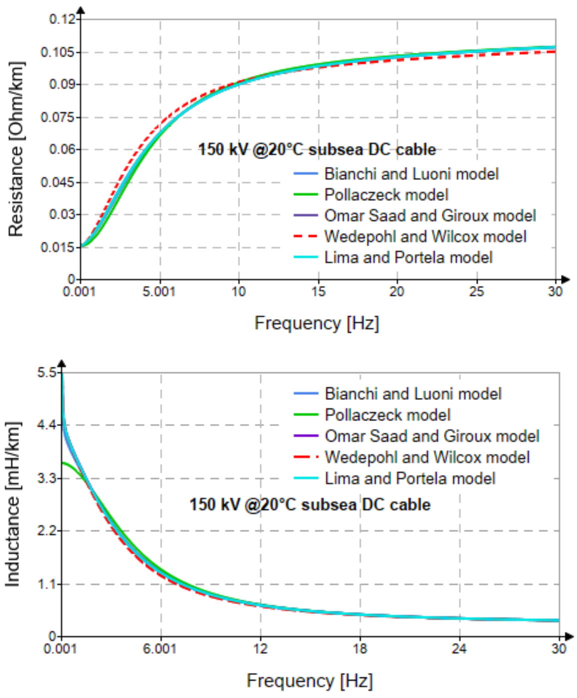

Fig.6. Resistance and inductance of DC cable (h = 100 m).

In order to provide additional references for correlating the calculated parameters of the DC cable at a frequency of 0.001 Hz, Table II shows the values obtained using other methods. This makes it possible to evaluate the level of adherence of results obtained through other methodologies. When comparing the results associated with the numerical models of the PSCAD and EMTP-RV software for the submarine DC cable, a good correlation between the electrical parameters is observed, despite the fact that they are estimated. Table II presents the resistance provided by the manufacturer ABB [15]. Once again, the consistency of the analysis methods for this parameter is reinforced.

Table II. – Electrical parameters of subsea DC cable

Models	150 kV @20°C, h~2500 m		
	R [Ω/km]	L [mH/km]	C [μF/km]
ABB datasheet	0.01510	-(*)	-(*)
Bianchi–Luoni	0.0152481	5.25562	0.23156
PSCAD (Wedepohl)	0.0152477	5.36599	0.23156
PSCAD (Omar Saad)	0.0152477	5.37021	0.23156
EMTP–RV (Pollaczeck)	0.0152473	5.43524	0.19113

(*) The values of the inductance and capacitance are not available.

It is important to note that the PSCAD software uses the Omar-Giroux and Wedepohl models to calculate DC cable impedance, while the EMPT-RV software uses Pollaczeck's approach for the same purpose. Given the demonstrated adherence of Saad's model with other models (see Figure 4), it is suitable to use Saad's model to calculate the electrical parameters of a subsea DC cable.

4. Conclusion

Within the scope established as the goal of the article, comparative analyses of the performance of several analytical models proposed in the literature were then carried out to determine the equivalent parameters of submarine cables. To this end, a physical construction structure of a 150 kV commercial submarine DC cable was used. Once the values of its parameters L, R, C were calculated, they were compared with values provided by the models available in the commercial software PSCAD and EMTP-RV. This correlation showed that the values obtained are consistent, a fact that indicates the consistency of the methods used. The most notable differences were observed in the low-frequency range. The same applies to frequencies above 10 Hz. Therefore, when considering the use of the cable for DC interconnections, the differences are of little relevance for the intended purposes. Despite the fact that the information provided by the manufacturer did not present values for inductance and equivalent capacitance, only resistance can be used for the purpose of evaluating theoretical information with a real cable. After the analysis carried out, it was found that the Wedepohl-Wilcox model is not suitable for calculating the impedance of DC cables operating at a depth of 2500 m. However, when carrying out the evaluations for depths of approximately 100 m, it was found that the Wedepohl-Wilcox model proved to be appropriate. This concludes that this strategy is suitable for shallow water scenarios or underground cables.

Acknowledgement

The authors would like to express their gratitude to the Brazilian oil and gas company – Petrobras, for their financial and technical support in making this article possible.

References

[1] Y. Ge, L. Xiang, Y. Li, R. He and W. Liu, "A novel topology for HVDC link connecting to offshore wind farms", IEEE International Conference on High Voltage Engineering and Application (2020), pp. 1-4.

[2] A. K. Biswas, S. I. Ahmed, S. K. Akula and H. Salehfar, "High Voltage AC (HVAC) and High Voltage DC (HVDC) Transmission Topologies of Offshore Wind Power and Reliability Analysis", IEEE Green Technologies Conference (2021), pp. 271-278

[3] Z. Li, R. Zhan, Y. Li, Y. He, J. Hou, X. Zhao and X. Zhang, "Recent developments in HVDC transmission systems to support renewable energy integration", Global Energy Interconnection. Vol. 1, pp. 595-607.

[4] A. Ray and K. Rajashekara, "Electrification of Offshore Oil and Gas Production: Architectures and Power Conversion", Energies (2023). Vol. 16.

[5] T. Dong, H. Brakelmann, "Analysis method for the design of long submarine cables", Renewable and Sustainable Energy Reviews (2023). Vol. 171.

[6] W. Wang, X. Yan, S. Li, L. Zhang, J. Ouyang, and X. Ni, "Failure of submarine cables used in high-voltage power transmission: Characteristics, mechanisms, key issues and prospects", IET Generation, Transmission & Distribution (2021).

[7] Z. Huang, J. A Pilgrim, P. Lewin, S. Swingler, and G. Tzemis, "Thermal modelling and analysis for offshore submarine high-voltage direct current cable crossings", IET Generation, Transmission & Distribution (2015).

[8] F. Pollaczeck, "Sur le champ produit par un conducteur simple infiniment long parcouru par un courant alternatif", Revue Gén, Elec (1931). Vol. 29, pp. 851-867.

[9] L. M. Wedepohl and D. J. Wilcox, "Transient analysis of underground power-transmission systems. System model and wave-propagation characteristics", Proc. IEE (1973). Vol. 120, pp. 253-260.

[10] O. Saad, G. Gaba and M. Giroux, "A Closed-Form Approximation for Ground Return Impedance of Underground Cables", IEEE Transactions on Power Delivery (1996). Vol. 11, pp. 1536-1545.

[11] A. Lima and C. Portela, "Closed-form expressions for ground return impedances of overhead lines and underground cables", International Journal of Electrical Power & Energy Systems (2012). Vol. 38, pp. 20-26.

[12] G. Bianchi and G. Luoni, "Induced currents and losses in single-core submarine cables", IEEE Transactions on Power Apparatus and Systems (1976). Vol. 95, pp. 49-58.

[13] C. H. Chien and R. W. G. Bucknall, "Analysis of Harmonics in Subsea Power Transmission Cables Used in VSC–HVDC Transmission Systems Operating Under Steady-State Conditions", IEEE Transactions on Power Delivery (2007). Vol. 22, pp. 2489-2497.

[14] S. Añó-Villalba, R. Blasco-Gimenez, S. Bernal-Perez, E. Belenguer, "Wind power plant integration in voltage source converter HVDC grids with voltage droop control", Mathematics and Computers in Simulation (2018). Vol. 146, pp. 186-199.

[15] ABB, Technical description of HVDC Light Technology, Elanders, Vasteras, POW-0038, rev. 5 ed., 2008.